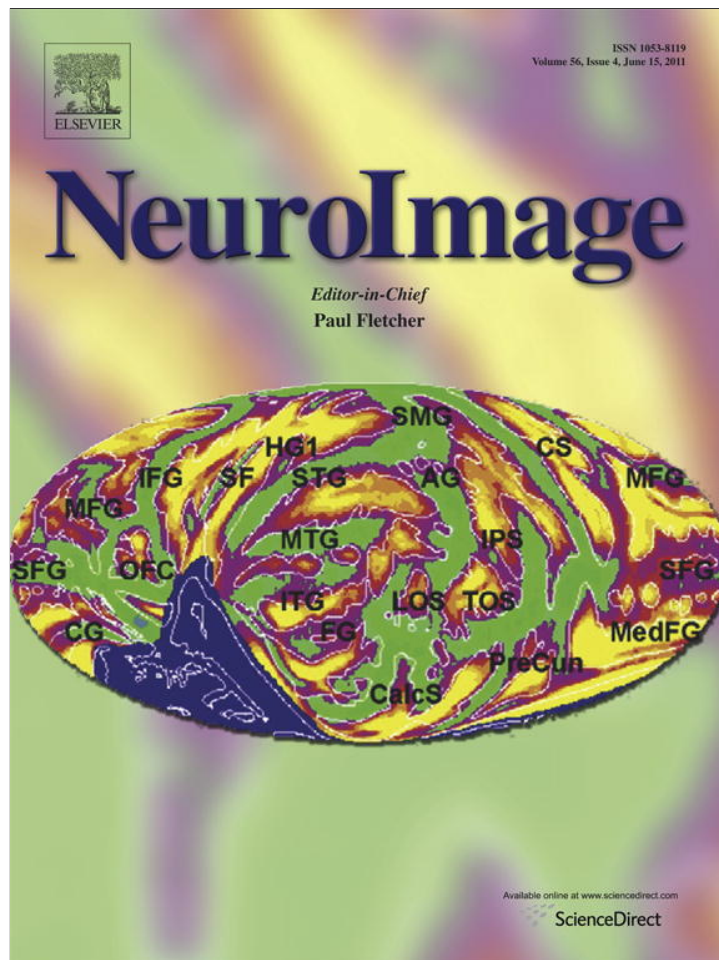


Provided for non-commercial research and education use.
Not for reproduction, distribution or commercial use.



This article appeared in a journal published by Elsevier. The attached copy is furnished to the author for internal non-commercial research and education use, including for instruction at the authors institution and sharing with colleagues.

Other uses, including reproduction and distribution, or selling or licensing copies, or posting to personal, institutional or third party websites are prohibited.

In most cases authors are permitted to post their version of the article (e.g. in Word or Tex form) to their personal website or institutional repository. Authors requiring further information regarding Elsevier's archiving and manuscript policies are encouraged to visit:

<http://www.elsevier.com/copyright>



Contents lists available at ScienceDirect

NeuroImage

journal homepage: www.elsevier.com/locate/ynimg

Common and dissociable neural correlates associated with component processes of inductive reasoning

Xiuqin Jia^{a,c,1}, Peipeng Liang^{a,b,c,1}, Jie Lu^{a,c}, Yanhui Yang^{a,c}, Ning Zhong^{b,c,d,*}, Kuncheng Li^{a,c,*}

^a Department of Radiology, Xuanwu Hospital, Capital Medical University, Beijing, China

^b The International WIC Institute, Beijing University of Technology, Beijing, China

^c Beijing Municipal Lab of Brain Informatics, Beijing, China

^d Department of Life Science and Informatics, Maebashi Institute of Technology, Maebashi, Japan

ARTICLE INFO

Article history:

Received 22 December 2010

Revised 28 February 2011

Accepted 7 March 2011

Available online 13 March 2011

ABSTRACT

The ability to draw numerical inductive reasoning requires two key cognitive processes, identification and extrapolation. This study aimed to identify the neural correlates of both component processes of numerical inductive reasoning using event-related fMRI. Three kinds of tasks: rule induction (RI), rule induction and application (RIA), and perceptual judgment (Jud) were solved by twenty right-handed adults. Our results found that the left superior parietal lobule (SPL) extending into the precuneus and left dorsolateral prefrontal cortex (DLPFC) were commonly recruited in the two components. It was also observed that the fronto-parietal network was more specific to identification, whereas the striatal-thalamic network was more specific to extrapolation. The findings suggest that numerical inductive reasoning is mediated by the coordination of multiple brain areas including the prefrontal, parietal, and subcortical regions, of which some are more specific to demands on only one of these two component processes, whereas others are sensitive to both.

© 2011 Elsevier Inc. All rights reserved.

Introduction

Inductive reasoning, a process of identifying the rule/pattern from instances, is considered as one of the most important higher cognitive functions of human brain. Number series completion, the typical inductive task, provides an important window onto inductive reasoning performance. The cognitive model of number series completion (with period length of one), is depicted as encoding, identification (including the stages of relation detection and completion of pattern description), extrapolation (including the stage of rule application), and answer production (Holzman and Pellegrino, 1983; Girelli et al., 2004). Actually, the identification and extrapolation are the two key cognitive components of number series completion task.

Identification refers to the process of rule induction, that is, to detect the relations between the elements to integrate the rule underlying the given number series. Several studies have found that dorsolateral prefrontal cortex (DLPFC) becomes increasingly activated when multiple relations need to be integrated in inductive reasoning (Christoff and Prabhakaran, 2001; Kroger et al., 2002; Goel and Dolan, 2004; Zhong et al., 2009). Brain lesion patients with damage to lateral prefrontal cortex are impaired in their ability to deal with relational integration problems (Waltz et al., 1999; Reverberi et al., 2005). In particular, our recent neuroimaging study has examined the importance of DLPFC in numerical

inductive reasoning, and suggests that the DLPFC is probably related to relational integration in identification process (Zhong et al., 2009). In that task, subjects were asked to draw the next number following a series, thus the reasoning process included both identification and extrapolation. However, the previous study focused on the neural correlates of whole processes of numerical inductive reasoning rather than the dissociable neural correlates of the two components. Thus it is difficult to explore whether the DLPFC is uniquely recruited in identification or it also has contribution to extrapolation.

Extrapolation refers to the process of rule application, that is, to apply the rule itself to the next element of the series. Functional imaging studies observe the activity of caudate region in inductive reasoning tasks (Christoff and Prabhakaran, 2001; Melrose et al., 2007). Melrose et al. (2007) design a figural series inductive reasoning task which includes both the identification and extrapolation processes within a single trial. However, due to their experimental conditions (e.g., reasoning task, reasoning control task, match task, and match control task), it is impossible to disengage the contribution of caudate to the rule induction and rule application processing. In addition, a study by Teichmann et al. (2005) indicates that the Huntington's disease (HD) patients with lesion in caudate/putamen are impaired in rule application including arithmetic. On the basis of previous evidence, we argued that the caudate could be more sensitive to extrapolation.

Despite of the existence of neuroimaging studies on the neural basis of inductive reasoning, no previous study has distinguished the neural correlates of identification and extrapolation component processes. Given this unsolved question, it is natural to consider whether

* Corresponding authors at: Beijing Municipal Lab of Brain Informatics, Beijing, China.
E-mail addresses: zhong@maebashi-it.ac.jp (N. Zhong), lkc1955@gmail.com (K. Li).

¹ Co-first authors: Xiuqin Jia and Peipeng Liang.

manipulation of identification and extrapolation processes recruits distinct, overlapped, or identical brain regions. Thus, the main goals of the present study were: 1) to explore the neural correlates of identification and examine whether the DLPFC is specially sensitive to demands on identification or additionally responds to the demands on extrapolation; 2) to explore the neural correlates of extrapolation and examine whether the striatum especially caudate is specific to rule application during extrapolation; and 3) to explore the spatial overlap or separability of neural correlates of identification and extrapolation component processes.

Materials and method

Subjects

Twenty paid healthy undergraduate and postgraduate students (10 females and 10 males) with the mean age of 23.60 ± 3.10 years, participated in the experiment. All subjects were right-handed and had the normal or corrected-to-normal vision. None of the subjects reported any history of neurological or psychiatric diseases. Written informed consent was obtained from each participant and this study was approved by the Ethics committee of Xuanwu Hospital, Capital Medical University.

Experimental design

Three types of experimental tasks: rule induction (RI), rule induction and application (RIA), and perceptual judgment (Jud) are showed in Table 1. For all tasks, there were three sequentially presented numbers. For the RI task (e.g., 13 15 17), subjects were required to identify the algorithm/rule (e.g., +2) underlying the given number series. For RIA tasks (e.g., 22 24 26), subjects were required to identify the rule (e.g., +2) and accordingly calculate the next number (e.g., 28). For the Jud task (e.g., 14 23 10), subjects were required to judge whether there was number 10 in the presented three numbers. Both RI and RIA tasks were half forward and half backward, and the carry/borrow position in the first two numbers or the last two numbers was balanced. Additionally, the distances between the correct and the false answer were less than 3. Half of Jud tasks contained the number 10 and half did not.

All the numbers involved in the number series and the answer were in the range of 1–99. The magnitude of arithmetic operation was between 2 and 9, and each magnitude had both forward and backward directions twice with different numbers. The magnitude of '1' (e.g., +1 or -1) and the counting series (e.g., 5 10 15) were excluded from the study. As stated in Holzman and Pellegrino (1983) and Lefevre and Bisanz (1986), several variables, such as type (e.g., addition, subtraction, multiplication, division), magnitude (e.g., +4 vs. +14) of arithmetic operation, period length of the pattern (e.g., rule +2: 3 5 7 vs. rule +1-3: 8 9 6 7 4) would influence inductive performance, thus, the abovementioned restrictions in the current designs would be helpful to reduce the heterogeneities within each kind of tasks and improve the comparability among different kinds of tasks.

To avoid the possibility that subjects acquired the rule of the RI and RIA tasks merely by the first two numbers without consideration of the third, additional 8 tasks for both RI and RIA, in which the relation between the first two numbers was different from that of the last two

numbers (e.g., 5 7 13), were designed to act as interferential tasks based on a pilot study. These interferential tasks were not employed in the data analysis. Except the interferential tasks, there were 32 trials for RI, 32 trials for RIA and 30 trials for Jud were used for the further data analysis.

As shown in Fig. 1, there were three sessions in the present study: RI session, RIA session and Jud session. Subjects were instructed the type of the session prior to the scanning. Within each session, stimuli were presented randomly in an event related design. The orders of the three sessions were counterbalanced among subjects. All the numbers were written with 36 pt "Times New Roman" font. Every trial began with the mark "+" in the center of the screen. The numbers appeared on the screen with the first number appearing at 2 s, the second at 2.6 s joining the first, and the last at 3.4 s joining the first two. The inter-stimulus interval (ISI) was 8 s. All numbers remained on the screen until button-press. Subjects were required to press the left or right button (counterbalanced among subjects) after the appearance of the third number when the answer was acquired. After that, two options were displayed, and subjects were instructed to select the answer by pressing one of the two buttons (left for "A", right for "B", or vice versa). Thus, the reaction time was acquired by the first button-press, and the accuracy was acquired by the second button-press. Subjects were instructed to respond as accurately and quickly as possible and move to the next trial if the stimuli advanced before they could respond.

MR data acquisition

Scanning was performed on a 3.0 T MRI system (Siemens Trio Tim; Siemens Medical System, Erlanger, Germany) and with a 12-channel phased array head coil. Foam padding and headphone were used to limit head motion and reduce scanning noise. High-resolution structural images were acquired using a T1 weighted 3D MPRAGE sequence (TR/TE = 1600/2.25 ms, TI = 800 ms, 192 sagittal slices, FOV = 256 mm, 9° flip angle, voxel size = 1 × 1 × 1 mm³). Functional images were obtained using a T2*gradient-echo EPI sequence (TR/TE = 2000/31 ms, 90° flip angle, 64 × 64 matrix size in 240 × 240 mm² FOV). Thirty axial slices with a thickness of 4 mm and an interslice gap of 0.8 mm were acquired and paralleled to the AC–PC line. The scanner was synchronized with the presentation of every trial.

Data preprocessing

fMRI data were preprocessed using SPM5 software (Wellcome Department of Cognitive Neurology, London, UK, <http://www.fil.ion.ucl.ac.uk>). The first four images were discarded in each session to allow the magnetization to approach dynamic equilibrium. Images were corrected for differences in timing of slice acquisition, followed by rigid body motion correction to the median image. The high resolution structural image was co-registered with the mean image of the EPI series. The structural image was then normalized to the MNI template, and normalization parameters were applied to EPI images. After

Table 1
Examples of experimental tasks.

Task	Options	Answer
RI	A. +2 B. +3	A
RIA	A. 30 B. 28	B
Jud	A. yes B. no	A

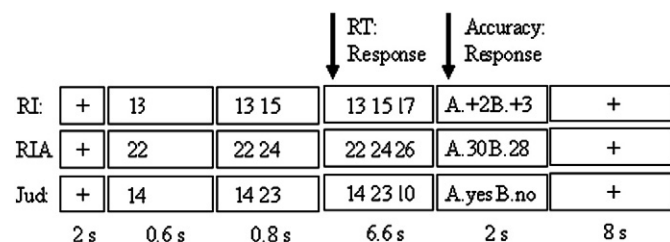


Fig. 1. Paradigm of stimuli presentation. The three numbers appeared within 2 s (i.e., 1 TR). If the subject made a response within 6.6 s (i.e., the first button-press) or 2 s (i.e., the second button-press), the remainder of the period was filled with a fixation period (the last 8 s). The reaction time (RT) was recorded by the first button-press, and the accuracy was recorded by the second button-press.

Table 2

Regions activated during identification component. The results were revealed by contrast of RI>Jud. Loci of maxima are in MNI coordinates in millimeters. The activations reported survived an uncorrected voxel-level intensity threshold of $p<0.001$ with a minimum cluster size of 15 contiguous voxels. SPL, superior parietal lobule; IFG, inferior frontal gyrus; MOG, middle occipital gyrus; MTG, middle temporal gyrus; PCC, posterior cingulate cortex; Parahip, parahippocampus; L, left; R, right. In order to directly observe the contribution of these regions, the list is ordered by the strength of activation of each cluster.

Region	BA	Cluster	MNI			T-score
			x	y	z	
L.SPL	7	138	-24	-63	45	6.94
L.Precuneus	7		-30	-51	51	4.93
	19		-24	-75	36	4.66
L.IFG	46	58	-45	33	15	6.91
			-42	42	9	5.64
L.MOG	19	174	-51	-57	-9	6.18
L.MTG	39		-45	-78	9	5.83
L.IFG	9	101	-48	9	33	5.71
			-36	3	30	4.36
R.MOG	19	60	42	-78	6	5.20
	18		30	-87	0	4.32
L.PCC	29	26	-3	-51	9	4.98
L.Parahip	30		-9	-42	0	4.17
R.SPL	7	27	30	-75	45	4.64
R.PCC	30	21	9	-54	6	4.58
R.Parahip	30		9	-42	0	4.34

normalization, all volumes were resampled into $3 \times 3 \times 3$ mm³ voxels. Head movement was <2 mm in all cases. fMRI data were then smoothed with an 8 mm FWHM isotropic Gaussian kernel.

fMRI analysis

Contrast images were constructed from each individual subject. On the group-level analysis a one-sample t-test was performed for each voxel of the contrast images. Only correctly answered trials were included in the analysis. The neural correlates of the identification component would be revealed by contrast of RI>Jud and the

Table 3

Regions activated during extrapolation component. The results were revealed by contrast of RIA>RI. Loci of maxima are in MNI coordinates in millimeters. The activations reported survived an uncorrected voxel-level intensity threshold of $p<0.001$ with a minimum cluster size of 15 contiguous voxels. SFG, superior frontal gyrus; MFG, middle frontal gyrus; MFC, medial frontal cortex; L, left; R, right. In order to directly observe the contribution of these regions, the list is ordered by the strength of activation of each cluster.

Region	BA	Cluster	MNI			T-score
			x	y	z	
<i>RIA-RI</i>						
L.Precuneus	19	88	-30	-78	33	7.20
L.Caudate		202	-12	18	12	5.94
L. medial globus pallidus			-9	3	-3	4.20
R.Thalamus		90	12	-21	12	5.91
			9	-21	-6	5.09
R.Caudate		168	15	18	6	5.74
R.Putamen			15	9	3	5.23
R.Cingulate	32	16	21	6	48	5.30
R.SFG	6		21	12	54	4.23
R.Precuneus	19	46	39	-81	36	5.26
L.Thalamus		52	-6	-12	9	5.22
L.MFG	6	40	-24	-9	48	5.11
			-30	3	51	4.20
L.MFG	6	54	-27	12	51	4.95
L.SFG	6		-24	6	57	4.65
L.MFC	32		-18	9	48	4.47
L.MFG	46	31	-48	27	24	4.92
			-42	33	18	4.11
L.Cingulate	32	23	-9	18	45	4.52
L.SFG	6		-3	12	57	4.36

Table 4

Common activation to identification and extrapolation components. The results were revealed by contrast of (RI>Jud) in conjunction with (RIA>RI). Loci of maxima are in MNI coordinates in millimeters. The activations reported survived an uncorrected voxel-level intensity threshold of $p<0.001$ with a minimum cluster size of 15 contiguous voxels. SPL, superior parietal lobule; MFG, middle frontal gyrus; L, left. In order to directly observe the contribution of these regions, the list is ordered by the strength of activation of each cluster.

Region	BA	Cluster	MNI			T-score
			x	y	z	
L.SPL	7	15	-24	-69	45	6.46
L.Precuneus	19		-24	-75	36	4.66
L.MFG	46	15	-45	33	18	6.20

extrapolation component by contrast of RIA>RI. Regions common to the identification and extrapolation components were revealed by contrast of RI>Jud in conjunction with RIA>RI. Regions specific to identification were revealed by contrast of RI>Jud exclusively masking RIA>RI, whereas regions specific to extrapolation were revealed by contrast of RIA>RI exclusively masking RI>Jud. For confirmation, additional three contrasts were also done: 1) contrast of RIA>Jud, which would yield regions activated during the whole process of inductive reasoning including identification and extrapolation components; 2) contrast of RI>Jud in conjunction with RIA>Jud, which would verify activation in the identification component; and 3) contrast of RIA>RI in conjunction with RIA>Jud, which would verify activation in the extrapolation component. The activations reported survived an uncorrected voxel-level intensity threshold of $p<0.001$ with a minimum cluster size of 15 contiguous voxels.

Definition of region of interest (ROI)

The ROIs (radius = 6 mm) were defined based on the exploratory results by WFU PickAtlas toolbox (<http://www.ansir.wfubmc.edu>). For each condition and each subject, a mean time-course, which represents the average intensity of the ROI, was computed across voxels in the ROI. BOLD responses of the ROIs reported throughout this paper were computed using the average response of the first two and the last two time points (scans) of a trial as the baseline from which percent change was calculated over the remaining time course of the trial.

Results

Behavioral performance

We performed ANOVAs on the accuracy (ACC) and reaction time (RT) of correct responses using RI, RIA and Jud as conditions. The average ACC was $97.97 \pm 3.09\%$ (mean \pm SD) for the RI task, $94.06 \pm 5.64\%$ for the RIA task, and $98.33 \pm 2.76\%$ for the Jud task. The main effect of condition was significant, $F(2, 38) = 6.610$, $p = 0.003$. Pairwise comparison analysis indicated that the ACC of RI and Jud was significantly higher than that of RIA task ($p = 0.007$, and $p = 0.013$, respectively). The difference between RI and Jud did not reach the significance.

The average RT was 803.04 ± 248.83 ms for the RI task, 1407.35 ± 513.02 ms for the RIA task, and 531.67 ± 114.51 ms for the Jud task. The main effect of condition was significant with $F(2, 38) = 61.295$, $p < 0.001$. Pairwise comparison analysis indicated that the RTs of RI and RIA were significantly longer than that of Jud ($p < 0.001$, and $p < 0.001$, respectively), and the RT of RIA was significantly longer than that of RI ($p < 0.001$). Additionally, the RT of the second button-press (i.e., from the presentation of the answer options to the response) was not significant between the three kinds of tasks (600.67 ± 77.68 ms for RI, 635.00 ± 127.98 ms for RIA, and 586.37 ± 92.33 ms for Jud).

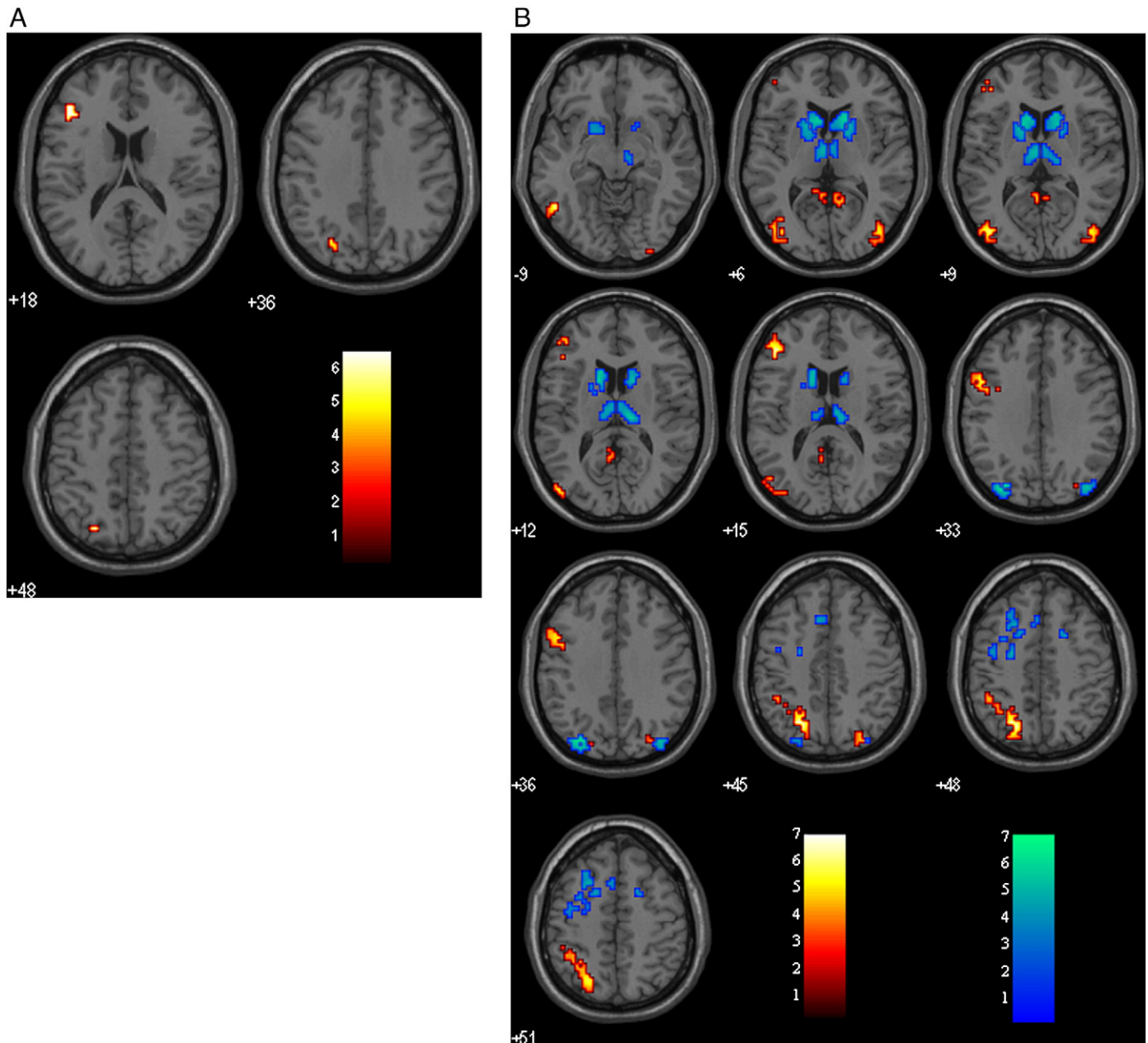


Fig. 2. Axial activation results from whole brain analysis (uncorrected $p < 0.001$, cluster size > 15 voxels, in MNI space). (A) Neural correlates common to identification and extrapolation components (revealed by the contrast of RI>Jud in conjunction with RIA>RI). Color bar indicates the t-score. (B) Neural correlates specific to identification component (revealed by the contrast of RI>Jud exclusively masking RIA>RI) and extrapolation component (revealed by the contrast of RIA>RI exclusively masking RI>Jud). Warm color bar indicates the t-scores specific to identification component, while winter color bar indicates the t-score specific to extrapolation component.

fMRI results

With regard to our experimental design, the RI task included the components of encoding, identification and answer production; the RIA task included additional extrapolation component besides the ones included in the RI task; and the Jud task mainly included the components of encoding and answer production. Thus, the identification and extrapolation components could be disentangled by the above defined contrasts.

Regions that showed increased activation during identification (RI>Jud, see Table 2) were found in the bilateral superior parietal lobule (SPL, L>R) extending to left precuneus, left dorsolateral prefrontal cortex (DLPFC, BA 46/9), as well as left occipitotemporal gyrus, right middle occipital gyrus, and bilateral posterior cingulate cortex (PCC) extend-

ing into parahippocampus. Regions that showed increased activation during extrapolation (RIA>RI, see Table 3) were found in the bilateral precuneus (BA 19, L>R), striatum (caudate, medial globus pallidus, and putamen), thalamus (R>L), as well as cingulate cortex, superior/middle frontal gyrus (L>R), and left DLPFC. It was hypothesized that the contrast of RIA>Jud would include the neural correlates of both identification and extrapolation processes. Thus, the neural correlates of identification (RI>Jud) should also be included in the contrast of RIA>Jud; similarly, the neural correlates of extrapolation (RIA>RI) should also be included in the contrast of RIA>Jud. In order to further confirm the results of identification and extrapolation components, additional analyses of conjunction were performed. The results showed that there was an identical activation pattern between the direct contrast (e.g., RI>Jud, or RIA>RI) and the additional conjunction analysis (e.g., RI>Jud in

Table 5

Activation specific to identification component. The results were revealed by contrast of [(RI>Jud) exclusively masking (RIA>RI)]. Loci of maxima are in MNI coordinates in millimeters. The activations reported survived an uncorrected voxel-level intensity threshold of $p < 0.001$ with a minimum cluster size of 15 contiguous voxels. SPL, superior parietal lobule; IPL, inferior parietal lobule; IFG, inferior frontal gyrus; MOG, middle occipital gyrus; MTG, middle temporal gyrus; PCC, posterior cingulate cortex; Parahip, parahippocampus; L, left; R, right. In order to directly observe the contribution of these regions, the list is ordered by the strength of activation of each cluster.

Region	BA	Cluster	MNI			T-score
			x	y	z	
L.SPL	7	123	-24	-63	45	6.94
L.Precuneus	7		-30	-51	51	4.93
L.IPL	40		-45	-42	48	4.44
L.IFG	46	41	-45	33	15	6.91
			-42	42	9	5.64
L.MOG	19	174	-51	-57	-9	6.18
L.MTG	39		-45	-78	9	5.83
L.IFG	9	90	-48	9	33	5.69
			-36	3	30	4.36
R.MOG	19	60	42	-78	6	5.20
	18		30	-87	0	4.32
L.PCC	29	26	-3	-51	9	4.98
L.Parahip	30		-9	-42	0	4.17
R.PCC	30	21	9	-54	6	4.58
R.Parahip	30		9	-42	0	4.34
R.SPL	7	22	27	-78	45	4.43

conjunction with RIA>Jud, or RIA>RI in conjunction with RIA>Jud) for identification [see [Supplementary data](#), [Tables S1, S2, S3g](#)] and extrapolation [see [Supplementary data](#), [Tables S1, S2, S4](#)], respectively.

The overlapped brain regions between identification and extrapolation components were determined by the contrast of RI>Jud in conjunction with RIA>RI (see [Table 4](#), [Fig. 2A](#)). These regions included the left superior parietal lobule extending into precuneus, and left DLPFC. Regions specific to identification were similar to activation during identification except reducing a few voxels in the SPL and left DLPFC (see [Table 5](#), [Fig. 2B](#)), which were determined by contrast of [(RI>Jud) exclusively masking (RIA>RI)]. Regions specific to extrapo-

Table 6

Activation specific to extrapolation component. The results were revealed by contrast of [(RIA>RI) exclusively masking (RI>Jud)]. Loci of maxima are in MNI coordinates in millimeters. The activations reported survived an uncorrected voxel-level intensity threshold of $p < 0.001$ with a minimum cluster size of 15 contiguous voxels. SFG, superior frontal gyrus; MFG, middle frontal gyrus; MFC, medial frontal cortex; L, left; R, right. In order to directly observe the contribution of these regions, the list is ordered by the strength of activation of each cluster.

Region	BA	Cluster	MNI			T-score
			x	y	z	
L.Precuneus	19	73	-30	-78	33	7.20
L.Caudate		202	-12	18	12	5.94
L.medial globus pallidus			-9	3	-3	4.20
R.Thalamus		90	12	-21	12	5.91
			9	-21	-6	5.09
R.Caudate		168	15	18	6	5.74
R.Putamen			15	9	3	5.23
R.Cingulate	32	16	21	6	48	5.30
R.SFG	6		21	12	54	4.23
R.Precuneus	19	41	39	-81	36	5.26
L.Thalamus		52	-6	-12	9	5.22
L.MFG	6	40	-24	-9	48	5.11
			-30	3	51	4.20
L.PreCG	6		-39	-9	48	4.19
L.MFG	6	51	-27	12	51	4.95
L.SFG	6		-24	6	57	4.65
L.MFC	32		-18	9	48	4.47
L.Cingulate	32	23	-9	18	45	4.52
L.SFG	6		-3	12	57	4.36

lation were found in the bilateral precuneus (BA 19, L>R), striatum (caudate, medial globus pallidus, and putamen), thalamus (R>L), as well as cingulate cortex, and superior/middle frontal gyrus (L>R) (see [Table 6](#), [Fig. 2B](#)), which were determined by contrast of [(RIA>RI) exclusively masking (RI>Jud)].

To show the pattern of the BOLD response, the first three strongest activated regions of identification and extrapolation were selected as ROIs. As to identification, [Fig. 3A](#) shows the percent signal change in the left SPL (BA 7, -24 -63 45), left DLPFC (BA 46, -45 33 15), and left MOG (BA 19, -51 -57 -9). In these ROIs, the differences in BOLD signal between RI and Jud were more evident than that of RIA and RI, that is, these regions mainly contributed to identification component. As to extrapolation, [Fig. 3B](#) shows the percent signal change in the left precuneus (-30 -78 33), left caudate (-12 18 12), and right thalamus (12-21 12). In these ROIs, the differences in BOLD signal between RIA and RI were more evident than that of RI and Jud, that is, these regions mainly contributed to extrapolation component.

Discussion

The present study is the first to jointly distinguish the neural correlates of identification and extrapolation. It was found that the left parietal area (SPL and precuneus) and left DLPFC were commonly engaged in identification and extrapolation. It was also observed that activations in the left fronto-parietal regions were more specific for identification, whereas activations in the striatal-thalamic regions were more specific for extrapolation.

Identification and the fronto-parietal network

A number of previous neuroimaging studies support the importance of DLPFC in inductive reasoning, for example, information integration ([Goel et al., 1997](#); [Goel and Dolan, 2004](#)), relation integration ([Christoff and Prabhakaran, 2001](#)), cognitive monitor ([Prabhakaran et al., 1997](#)), retrieval of rule knowledge ([Geake and Hansen, 2005](#)), and access to world knowledge ([Goel and Dolan, 2004](#); [Liang et al., 2007](#)). [Reverberi, et al. \(2005\)](#), present a rule generation and recognition test to patients and find that the left lateral prefrontal lesion subgroup failed to generate hypotheses (rule induction) even normally on the rule recognition test. Another neuropsychological evidence shows that patients with damage to prefrontal cortex exhibit deficit in reasoning tasks requiring the integration of multiple relations (2-relational); whereas they perform normally for 0- and 1-relational tasks, and also for episodic and semantic memory tasks ([Waltz et al., 1999](#)). Although there was partially overlapped activation in DLPFC during the two component processes as the common processes of working memory involved in them, there was greater brain activity in DLPFC that is more specific to the identification component. In the present study, the identification component also required to integrate relations between numerical items (e.g., 13 15 17). The present findings add to previous evidence that the DLPFC is selectively engaged by the need to integrate relations to reason.

The superior parietal lobule, near the intraparietal sulcus, has been reported to be activated in figural inductive reasoning adapted from Raven's Progressive Matrices ([Christoff and Prabhakaran, 2001](#); [Kroger et al., 2002](#); [Prabhakaran et al., 1997](#)). Neuroimaging studies of number comparison ([Pinel et al., 2001](#); [Cohen Kadosh et al., 2005](#)), approximation ([Dehaene et al., 1999](#); [Stanescu-Cosson et al., 2000](#)), arithmetic operation ([Ischebeck et al., 2006](#); [Lee, 2000](#)), and counting ([Piazza et al., 2002](#)), all report activity in SPL during these tasks. [Dehaene et al. \(1993\)](#), point out that the semantic representation of numerical magnitude can be regarded as to an internal "number line", and the covert attention is engaged when attending to present specific quantities on the number line. The overlapped activity in SPL for identification and extrapolation components might reflect the number representation in the "number line" and arithmetic operation, such as, identifying the rule of + 2 for identification, and applying the rule to

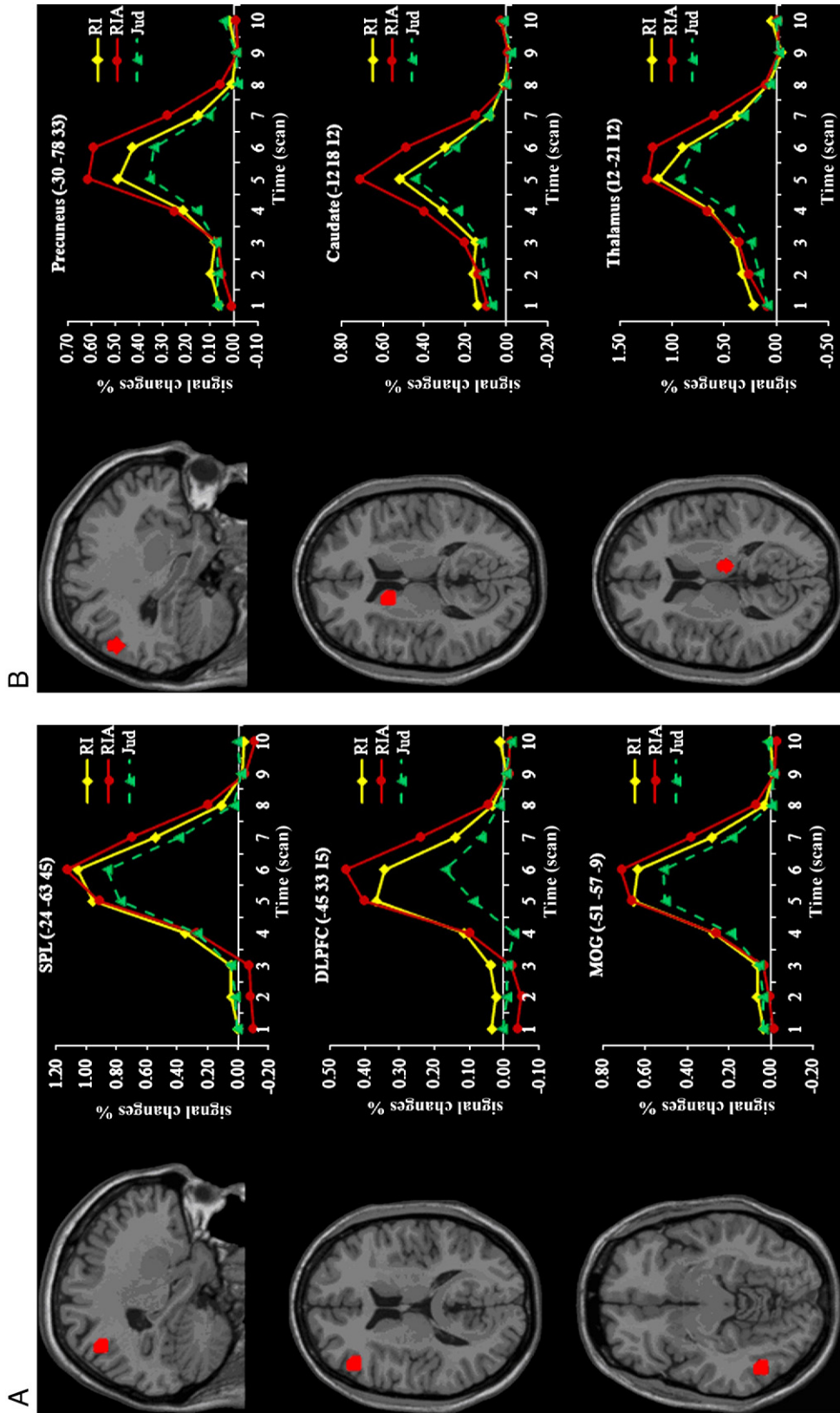


Fig. 3. Time courses of the percent signal changes from the ROIs. (A) ROIs of identification component. Significant BOLD signal changes appeared for identification component (RI>Jud) and no significant change for extrapolation component (RIA>RI) in the ROIs of SPL (-24 -63 45), DLPFC (-45 33 15) and MOC (-51 -57 -9). (B) ROIs of extrapolation component. Significant BOLD signal changes appeared for extrapolation component (RIA>RI) and no significant change for identification component (RI>Jud) in the ROIs of precuneus (-30 -78 33), caudate (-12 18 12) and thalamus (12-21 12). Coordinate was in the MNI space.

produce the next number $26 + 2 = 28$ for extrapolation. Furthermore, neuroimaging studies of number comparison have consistently found activation in the intraparietal sulcus when subjects were required to decide which quantity was larger (Pinel et al., 2001; Gobel et al., 2004). In line with previous studies, more brain activity in SPL specific to identification, might relate to comparison between numerical items (e.g., 13 15 17) in order to detect the relation (e.g., +2) among them.

In addition, identification process also needed other brain regions, such as the occipitotemporal and occipital areas. Seger and Cincotta (2002), have found that occipital region activated during implicit concept learning (including rule induction component), but not during explicit concept learning. The activation pattern of occipital region implies that the task involving implicit rule identification had greater covert attention/visual processing demands during identification than the extrapolation process. Indeed during the extrapolation participants just applied the identified rule to the next number, whereas during identification, participants had to pay more attention to each number item in order to discover the implicit rule among the stimuli.

Extrapolation and the striatal–thalamic network

Previous animal studies (Berendse and Groenewegen, 1990; Cheatwood et al., 2003) and primate studies (Fenelon et al., 1991; Sidibe and Smith, 1999), have demonstrated that the thalamic information is conveyed to striatal neurons (thalamic neurons projecting to striatum). In the present study, we found activation in striatal–thalamic network specific to extrapolation component. Patients with degenerative striatum such as Huntington's disease (HD) show deficits in rule application including arithmetic operation (Teichmann et al., 2005). In the present study, the extrapolation process required to apply the rule to generate the next number, e.g., applying the rule +2 to the sequence of 22 24 26 and producing the answer 28. In line with previous study (e.g., Teichmann et al., 2005), this study explored the greater activation in striatal regions specific to extrapolation rather than identification during numerical inductive reasoning. Moreover, our previous study also outlines the important role of striatal–thalamic network in figural inductive reasoning (Mei et al., 2010). Thus, the striatal–thalamic network was the important component of the neural system mediating the neural activity of extrapolation process of inductive reasoning.

In addition, several neuroimaging studies have found significant activation of the precuneus during non-imageable tasks, and suggested the role in successful episodic memory retrieval irrespective of the process of mental imagery, for example, a paired word associate memory with abstract nouns and musical episodic memory (for a review, see Cavanna and Trimble, 2006). In line with previous studies, we found that strongest activation in precuneus was during extrapolation which required successful retrieval of the identified rule. Thus, activation of the precuneus might exhibit the strong correlation with successful retrieval of remembered rules.

Conclusion

The present study was able to provide new insights into the neural architecture of the component mechanisms underlying numerical inductive reasoning. Our findings show that the two key components of inductive reasoning, identification and extrapolation, are associated with the coordination of activity in multiple, functionally dissociable regions. These regions include those that are sensitive to demand on one component process, as well as regions that are jointly activated by both identification and extrapolation, mapping onto common and dissociable components of cognitive control required for identification and extrapolation during numerical inductive reasoning.

Acknowledgments

This work was supported by the Open Research Fund of the State Key Laboratory of Cognitive Neuroscience and Learning (no. CNKOPZD1001), China Postdoctoral Science Foundation funded project (no. 201003142), and the State Key Program of National Natural Science of China (no. 30930029).

Appendix A. Supplementary data

Supplementary data to this article can be found online at doi:10.1016/j.neuroimage.2011.03.020.

References

- Berendse, H.M., Groenewegen, H.J., 1990. Organization of the thalamostriatal projections in the rat, with special emphasis on the ventral striatum. *J. Comp. Neurol.* 299 (2), 187–228.
- Cavanna, A.E., Trimble, M.R., 2006. The precuneus: a review of its functional anatomy and behavioural correlates. *Brain* 129, 564–583.
- Cheatwood, J.L., Reep, R.L., Corwin, J.V., 2003. The associative striatum: cortical and thalamic projections to the dorsocentral striatum in rats. *Brain Res.* 968 (1), 1–14.
- Christoff, K., Prabhakaran, V., 2001. Rostrolateral prefrontal cortex involvement in relational integration during reasoning. *Neuroimage* 14 (5), 1136–1149.
- Cohen Kadosh, R., Henik, A., Rubinsten, O., Mohr, H., Dori, H., van de Ven, V., Zorzi, M., Hendler, T., Goebel, R., Linden, D.E., 2005. Are numbers special? The comparison systems of the human brain investigated by fMRI. *Neuropsychologia* 43, 1238–1248.
- Dehaene, S., Bossini, S., Giraux, P., 1993. The mental representation of parity and numerical magnitude. *J. Exp. Psychol. Gen.* 122, 371–396.
- Dehaene, S., Spelke, E., Stanescu, R., Pinel, P., Tsivkin, S., 1999. Sources of mathematical thinking: Behavioral and brain-imaging evidence. *Science* 284, 970–974.
- Fenelon, G., Francois, C., Percheron, G., Yelnik, J., 1991. Topographic distribution of the neurons of the central complex and of other thalamic neurons projecting to the striatum in macaques. *Neuroscience* 45 (2), 495–510.
- Geake, J.G., Hansen, P.H., 2005. Neural correlates of intelligence as revealed by fMRI of fluid analogies. *Neuroimage* 26 (2), 555–564.
- Girelli, L., Semenza, C., Delazer, M., 2004. Inductive reasoning and implicit memory: evidence from intact and impaired memory systems. *Neuropsychologia* 42, 926–938.
- Gobel, S.M., Johansen-Berg, H., Behrens, T., Rushworth, M.F.S., 2004. Response-selection-related parietal activation during number comparison. *J. Cogn. Neurosci.* 16 (9), 1536–1551.
- Goel, V., Gold, B., Kapur, S., Houle, S., 1997. The seats of reason? An imaging study of deductive and inductive reasoning. *Neuroreport* 8 (5), 1305–1310.
- Goel, V., Dolan, R.J., 2004. Differential involvement of left prefrontal cortex in inductive and deductive reasoning. *Cognition* 93 (3), B109–B121.
- Holzman, T.G., Pellegrino, J.W., 1983. Cognitive variables in series completion. *J. Educ. Psychol.* 75 (4), 603–618.
- Ischebeck, A., Zamarian, L., Siedentopf, C., Koppelstätter, F., Benke, T., Felber, S., Delazer, M., 2006. How specifically do we learn? Imaging the learning of multiplication and subtraction. *Neuroimage* 30, 1365–1375.
- Kroger, J.K., Sabb, F.W., False, C.L., Bookheimer, S.Y., Cohen, M.S., Holyoak, K.J., 2002. Recruitment of anterior dorsolateral prefrontal cortex in human reasoning: a parametric study of relational complexity. *Cereb. Cortex* 12, 477–485.
- Lee, K.M., 2000. Cortical areas differentially involved in multiplication and subtraction: a functional magnetic resonance imaging study and correlation with a case of selective acalculia. *Ann. Neurol.* 48, 657–661.
- Lefevre, J.-A., Bisanz, J., 1986. A cognitive analysis of number-series problems: sources of individual differences in performance. *Mem. Cogn.* 14 (4), 287–298.
- Liang, P.P., Zhong, N., Lu, S.F., Liu, J.M., Yao, Y.Y., Li, K.C., Yang, Y.H., 2007. The neural mechanism of human numerical inductive reasoning process: a combined ERP and fMRI study. *LNAI* 4845, 223–243.
- Mei, Y., Liang, P.P., Lu, S.F., Yang, Y.H., Zhong, N., Li, K.C., 2010. Neural mechanism of figural inductive reasoning: An fMRI study. *Acta Psychol. Sin.* 42 (4), 1–11.
- Melrose, R.J., Poulin, R.M., Stern, C.E., 2007. An fMRI investigation of the role of the basal ganglia in reasoning. *Brain Res.* 1142, 146–158.
- Piazza, M., Mechelli, A., Butterworth, B., Price, C.J., 2002. Are subitizing and counting implemented as separate or functionally overlapping processes? *Neuroimage* 15, 435–446.
- Pinel, P., Dehaene, S., Riviere, D., LeBihan, D., 2001. Modulation of parietal activation by semantic distance in a number comparison task. *Neuroimage* 14, 1013–1026.
- Prabhakaran, V., Smith, J.A.L., Desmond, J.E., Glover, G.H., Gabrieli, J.D.E., 1997. Neural substrates of fluid reasoning: an fMRI study of neocortical activation during performance of the Raven's Progressive Matrices Test. *Cognit. Psychol.* 33, 43–63.
- Reverberi, C., D'Agostini, S., Skrap, M., Shallice, T., 2005. Generation and recognition of abstract rules in different frontal lobe subgroups. *Neuropsychologia* 43, 1924–1937.
- Seger, C.A., Cincotta, C.M., 2002. Striatal activity in concept learning. *Cogn. Affect. Behav. Neurosci.* 2 (2), 149–161.
- Sidibe, M., Smith, Y., 1999. Thalamic inputs to striatal interneurons in monkeys: synaptic organization and co-localization of calcium binding proteins. *Neuroimage* 89 (4), 1189–1208.
- Stanescu-Cosson, R., Pinel, P., van De Moortele, P.F., Le Bihan, D., Cohen, L., Dehaene, S., 2000. Understanding dissociations in dyscalculia, a brain imaging study of the

- impact of number size on the cerebral networks for exact and approximate calculation. *Brain* 123, 2240–2255.
- Teichmann, M., Dupoux, E., Kouider, S., Brugieres, P., Boisse, M.-F., Baudic, S., Cesaro, P., Peschanski, M., Bachoud-Levi, A.-C., 2005. The role of the striatum in rule application: the model of Huntington's disease at early stage. *Brain* 128, 1155–1167.
- Waltz, J.A., Knowlton, B.J., Holyoak, K.J., Boone, K.B., Mishkin, F.S., de Menezes Santos, M., Thomas, C.R., Miller, B.L., 1999. A system for relational reasoning in human prefrontal cortex. *Psychol. Sci.* 10 (2), 119–125.
- Zhong, N., Liang, P.P., Qin, Y.L., Lu, S.F., Yang, Y.H., Li, K.C., 2009. Neural substrate of data-driven science discovery: an fMRI study. *Sci. China C Life Sci.* 39 (3), 271–278.